Hindawi
Journal of Chemistry
Volume 2018, Article ID 5608243, 7 pages
https://doi.org/10.1155/2018/5608243

Research Article

An Effective Pt-Cu/SiO_2 Catalyst for the Selective Hydrogenation of Cinnamaldehyde

Dong Wang[1] and Yujun Zhu[2]

[1]*School of Chemical and Environmental Engineering, Hanshan Normal University, Chaozhou 521041, China*
[2]*Key Laboratory of Functional Inorganic Material Chemistry, Ministry of Education, School of Chemistry and Materials, Heilongjiang University, Harbin 150080, China*

Correspondence should be addressed to Yujun Zhu; yujunzhu@hlju.edu.cn

Received 14 December 2017; Accepted 18 March 2018; Published 24 April 2018

Academic Editor: Ioannis D. Kostas

The bimetal catalyst Pt-Cu/SiO_2 was prepared by the impregnation method. Its catalytic performance was investigated by the selective hydrogenation of cinnamaldehyde. Pt-Cu/SiO_2 exhibited much higher selectivity (64.1%) to cinnamyl alcohol than Pt/SiO_2 (3.7%), while they showed similar conversion of cinnamaldehyde. This enhancement was attributed to the increase in the amount of the Pt^0 species on the Pt-Cu/SiO_2 surface, which is derived from the interaction between Pt and Cu revealed by XRD and XPS.

1. Introduction

Selective catalytic hydrogenation of α,β-unsaturated aldehydes is an important step in industrial production of fine chemicals, such as pharmaceuticals, flavours, and fragrances [1–5]. Cinnamaldehyde (CAL) is representative α,β-unsaturated aldehydes, which can be hydrogenated first via C=C or C=O double bonds to hydrocinnamaldehyde (HALD) or cinnamyl alcohol (COL), followed by total hydrogenation of these products to hydrocinnamyl alcohol (HALC) (Scheme 1) [1]. In general, the reduction of the C=C group is favored thermodynamically [1, 2]. Thus, it is still a challenging task to enhance the selectivity for the hydrogenation of C=O group to form COL [2, 6, 7].

Nowadays, Pt-based catalyst facilitates the production of COL via the hydrogenation of the C=O bond [8–12]. The unique advantage of such catalysts is that activity and selectivity can be tuned by controlling the size, shape, and surface species of Pt particles [1, 13–15]. In fact, many methods have been developed to enhance the performance of Pt-based catalyst, such as investigating novel support and promoter [15–19]. In our previous works, it was found that graphene-supported Pt catalysts showed high selectivity to COL [13]; and the activity and selectivity of Pt/carbon nanosheets (CNS) catalysts increased with the rise of the graphitization degree of CNS [20]. Moreover, the selectivity of Pt catalyst does not depend on particle size, at least within the 1.5–2.5 nm particle size range over Pt/SiO_2 [21]. We also found that Mo_2N could enhance the efficiency of Pt on ternary catalyst Pt-Mo_2N/SBA-15 due to the synergistic effect of Pt and Mo_2N [22]. Furthermore, some other studies illustrated that the introduction of a second metal promoter was also a valid way to improve the catalytic properties of Pt nanoparticles. It has been reported that metal promoters (Ga, Fe, Ni, and Ru) play an important role in CAL hydrogenation [7, 23, 24].

In light of the above, a thought stimulates us to investigate whether the nonnoble metal of Cu could promote the catalytic performance of Pt for the hydrogenation of cinnamaldehyde. Thus, the Pt-Cu bimetal catalyst on SiO_2 aerogel (Pt-Cu/SiO_2) was prepared by a simple impregnation method, and its performance on selective hydrogenation of cinnamaldehyde was investigated. To our delight, the Pt-Cu/SiO_2 catalyst showed much higher selectivity than Pt/SiO_2. It was found that the addition of Cu enhanced the dispersion of Pt on SiO_2. Moreover, there were more Pt^0 species on bimetal catalyst, which benefitted the enhancement of the selectivity to COL.

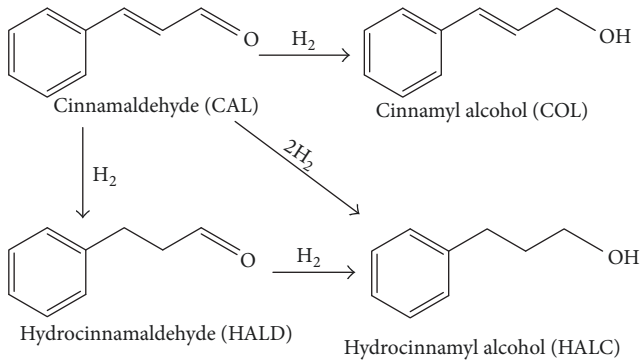

Scheme 1: Hydrogenation products of cinnamaldehyde.

2. Material and Method

2.1. Catalyst Preparation. SiO_2 aerogel was purchased from Aladdin. Bimetal catalyst was synthesized by impregnation and hydrogen reduction method. Firstly, 0.4 g $Cu(NO_3)_2{\cdot}3H_2O$ was dissolved in 20 mL water at room temperature, and then 2 mol/L ammonia water was dropped to the mixture until there was no precipitation. Secondly, 1.00 g SiO_2 aerogel was added to the above solution. After stirring for 4 h, the blue powder was collected by filtration and washing and dried at 80°C. Thirdly, 0.300 g blue powder was impregnated with 1.5 mL H_2PtCl_6 (10 mmol/L) ethanol solution. The resulting suspension was stirred at room temperature to remove the solvent and dried at 80°C for 12 h. Finally, the sample was placed inside a furnace with a heating rate of 5°C min^{-1} to 300°C under N_2 atmosphere which was maintained at 300°C for 1 h under pure H_2 atmosphere. Thus, the obtained sample was denoted as Pt-Cu/SiO_2. As references, Pt supported on SiO_2 aerogel sample was also prepared under similar condition, which was denoted as Pt/SiO_2.

2.2. Catalyst Characterization. The X-ray diffraction (XRD) patterns were performed by using a Bruker D8 Advance X-ray diffractometer with Cu Kα (λ = 1.5418 Å) radiation (40 kV, 40 mA). The scan range of the wide-angle XRD was 10–80°. Based on XRD results, the average particles sizes can be calculated from Pt(111) by Scherrer's equation. The average particles sizes were recalculated to dispersion values assuming spherical shapes and using the formula described by Scholten et al.:

$$D = 10^{21} \times \frac{6 \times M \times \rho_{\text{site}}}{d \times \rho_{\text{metal}} \times N}. \quad (1)$$

D is dispersion ($Pt_{surface}/Pt_{total}$), M is the atomic weight (195.1 g/mol for Pt), ρ_{site} is the platinum surface site density (12.5 Pt atoms/nm^2), d is particle size (nm), ρ_{metal} is the metal density (21.45 g/cm^3 for Pt), and N is the Avogadro constant. Thus, $D = 1.13/d$ (nm) for Pt [25, 26].

Properties of surface area were derived from N_2 adsorption-desorption isotherms at 77 K with a Micromeritics Tristar II surface area and a porosimetry analyzer. Before the measurement, samples were degassed under vacuum at 150°C for 5 h. The surface area was determined from desorption isotherms by the BET method.

The morphology and structure of the samples were analyzed by using a JEM-2100 transmission electron microscopy (TEM) with an acceleration voltage of 200 kV.

X-ray photoelectron spectroscopy (XPS) was conducted on a Kratos-AXIS ULTRA DLD with an AlKα radiation source. Binding energies (BE) refer to the C (1s) binding energy of carbon taken to be 284.7 eV.

The content of Pt and Cu on the Pt-Cu/SiO_2 catalyst was determined by inductively coupled plasma-optical emission spectrometry (ICP-OES), which was performed by using a PerkinElmer Optima 7000DV analyzer. Each sample was dissolved in a diluted HF and chloroazotic acid solution before measurement.

2.3. Selective Hydrogenation of Cinnamaldehyde. The catalyst (50 mg) was mixed with 1.00 g CAL and 30 mL isopropanol. The mixture was subsequently transferred to a 100 mL autoclave. After flushing three times with N_2 at 5 bar and three times with H_2 at 5 bar, the reaction was allowed to proceed at 80°C under 10 bar of H_2 for 2 h.

The products were analyzed by GC (Agilent 7820 A) with flame ionization detection (FID) and a HP-5 capillary column (30 m × 0.32 mm × 0.25 mm). Quantitative analysis of the products was performed via calibration curves using the benzyl alcohol as an external standard. The products were further identified by GC-MS (Agilent 6890/5973N).

3. Results and Discussion

3.1. Characterization of Catalysts. Figure 1 shows the XRD patterns of SiO_2, Pt/SiO_2, and Pt-Cu/SiO_2 samples. All of them displayed a diffuse peak of amorphous SiO_2 around 22.5°. For Pt/SiO_2, a series of characteristic diffraction lines of platinum at 39.5, 46.4, and 67.4° were observed, which was identified as the (111), (200), and (220) reflections of Pt with face-centered cubic structure [22]. According to Scherrer's equation, the grain size of Pt nanoparticles on the Pt/SiO_2 sample was about 21.54 nm (Table 1). Compared with the Pt diffraction peak of the Pt/SiO_2 sample, the Pt (111) diffraction peak of the Pt-Cu/SiO_2 sample becomes broadened and shifts to 41.1°, and the reflection of Pt (200) and (220) apparently disappears. Meanwhile, the diffraction peaks assigned to the Cu species are not observed, which may be ascribed to the little amount of Cu (0.33 wt%, Table 1) measured by ICP.

Comparing the XRD patterns of the Pt-Cu/SiO_2 (Figure 1(c)) with those of the Pt/SiO_2 (Figure 1(b)), on one hand, the broadening peak of Pt (111) and the disappearance of the Pt (200) and Pt (220) peaks for the Pt-Cu/SiO_2 imply that the addition of Cu is able to decrease the size of Pt particles and improve the dispersion of Pt. In view of the calculation using Scherrer's equation, the Pt particle size for the Pt-Cu/SiO_2 sample (11.05 nm) was much smaller than that of the Pt/SiO_2 (21.54 nm), which also implies that the addition of Cu benefits gaining relatively small Pt particles. On the other hand, the diffraction peak of the Pt (111) shifted to higher angle with the addition of Cu. It is likely that the Cu atom is incorporated into the crystal lattice of Pt and then occupies the position of

Table 1: Physicochemical properties of Pt-Cu/SiO_2 catalysts.

Sample	S_{BET} (m^2/g)[a]	Pt loading (wt%)[b]	Cu loading (wt%)[b]	$\bar{d}$XRD (nm)[c]	$\bar{d}$TEM (nm)[d]	D(Pt) (%)[e]
SiO_2	550	-	-	-	-	
Pt/SiO_2	364	1.21	-	21.54	-	5.24
Pt-Cu/SiO_2	410	1.14	0.33	11.05	10.25	10.22

[a]Derived from nitrogen adsorption-desorption isotherm. [b]The contents of Pt and Cu are tested by ICP-OES. [c]Average particle sizes calculated from XRD patterns of Pt based on Scherrer's equation. [d]Average particle sizes calculated from at least 50 individual crystallites in TEM images. [e]Estimated from the mean particle size of Pt calculated from XRD patterns.

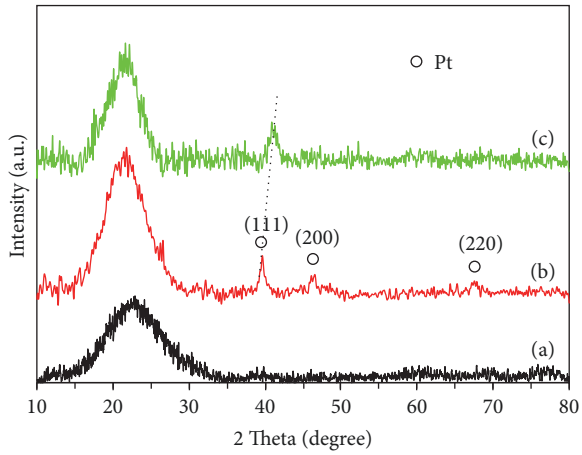

Figure 1: Wide-angle XRD patterns of (a) SiO_2, (b) Pt/SiO_2, and (c) Pt-Cu/SiO_2.

Pt atoms. The atomic radius of Cu (0.128 nm) is a little smaller than Pt (0.139 nm); the substitution of Cu for Pt results in the crystal cell of Pt shrinking and the parameters of crystal cell decreasing. The difference of XRD patterns illustrates that there are interactions between Pt and Cu in the Pt-Cu/SiO_2 sample.

The textural properties of the samples were investigated by N_2 adsorption-desorption isotherms. The BET specific surface area is summarized in Table 1. It was worthwhile to note that the surface area significantly decreased after metal modification. The BET surface area of the Pt/SiO_2 decreased to 364 $m^2\,g^{-1}$ from 550 $m^2\,g^{-1}$ for SiO_2. For the Pt-Cu/SiO_2, the corresponding surface area decreased to 410 $m^2\,g^{-1}$. This indicated that Pt and Cu were loaded on the SiO_2 support and occupied its surface. According to the results revealed by XRD patterns, the particle size of Pt-Cu/SiO_2 was smaller than that of Pt/SiO_2; therefore the surface area of the Pt-Cu/SiO_2 was slightly larger than that of the Pt/SiO_2.

Figure 2 shows the TEM images of Pt/SiO_2 and Pt-Cu/SiO_2. Unfortunately, we failed to take the HRTEM images of the samples, maybe due to the wrapping of SiO_2 aerogel. From Figures 2(a)–2(c), it can be seen that the dispersion of Pt nanoparticles on Pt/SiO_2 catalysts was poor. The Pt nanoparticles size was not uniform, and the aggregation is serious (Figure 2(b)). Thus, it is difficult to gain its average particle size determined by statistical analysis. With regard to the Pt-Cu/SiO_2 sample in Figures 2(d)-2(e), the Pt nanoparticles were highly dispersed on SiO_2 supporter with uniform size ($\langle d\rangle = 10.25 \pm 0.30$ nm), which was in line with the XRD results. Although the average particle size of the Pt/SiO_2 was not available, it is obvious that the Pt-Cu/SiO_2 sample exhibits much smaller particle size and far better dispersion. The observations disclose that the addition of Cu helps to disperse Pt and effectively avoids agglomeration of Pt.

XPS was conducted to investigate the surface properties and the chemical states of Pt. Figure 3 shows the Pt 4f XPS of Pt/SiO_2 and Pt-Cu/SiO_2 together with corresponding deconvolution by fitting Gaussian peaks after Shirley-background subtraction. As shown in Figure 3, the Pt XPS of Pt/SiO_2 and Pt-Cu/SiO_2 presented a doublet corresponding to Pt $4f_{7/2}$ and Pt $4f_{5/2}$, and the corresponding binding energy (BE) is listed in Table 2. As for the Pt/SiO_2 sample, the Pt $4f_{7/2}$ BE at 71.14 eV was ascribed to platinum in the metallic state (Pt^0); the Pt $4f_{7/2}$ peak around 73.34 eV could be assigned to the Pt^{2+} species and the Pt $4f_{7/2}$ peak at 75.52 eV was attributed to the Pt^{4+} species. But there were only two kinds of Pt species in the Pt-Cu/SiO_2 sample. As shown in Figure 3(b), the peak located at 70.93 eV was attributed to Pt^0, while the peak around 72.99 eV corresponded to the Pt^{2+} species. Interestingly, the BE of Pt^0 and Pt^{2+} species for the Pt-Cu/SiO_2 sample exhibited a negative shift compared with that for Pt/SiO_2 sample. This shift should be attributed to the electrons transfer from Cu to Pt by their intimate contact. In other studies [10, 11, 22, 23, 28], this electron transfer phenomenon between precious and promoter was also found, and the direction of this transfer changed with the nature of precious metal and promoter.

Furthermore, what is noticeable is the difference in the quantitation of the surface Pt species. As listed in Table 2, Pt^0, Pt^{2+}, and Pt^{4+} species simultaneously existed in the Pt/SiO_2 sample and the corresponding proportion was 28%, 53%, and 19%, respectively. Obviously, for the Pt/SiO_2, metal Pt exists mostly in the form of the Pt^{2+} species.

As far as the Pt-Cu/SiO_2 was concerned, there were only Pt^0 and Pt^{2+} species, and the ratios were 60% and 40%, respectively. Compared with the Pt/SiO_2, the Pt-Cu/SiO_2 contains more Pt^0 content and less Pt^{4+} amount. This suggests that the strengthening of metallic characteristics of Pt in Pt-Cu/SiO_2 may be attributed to the presence of the transition metal Cu.

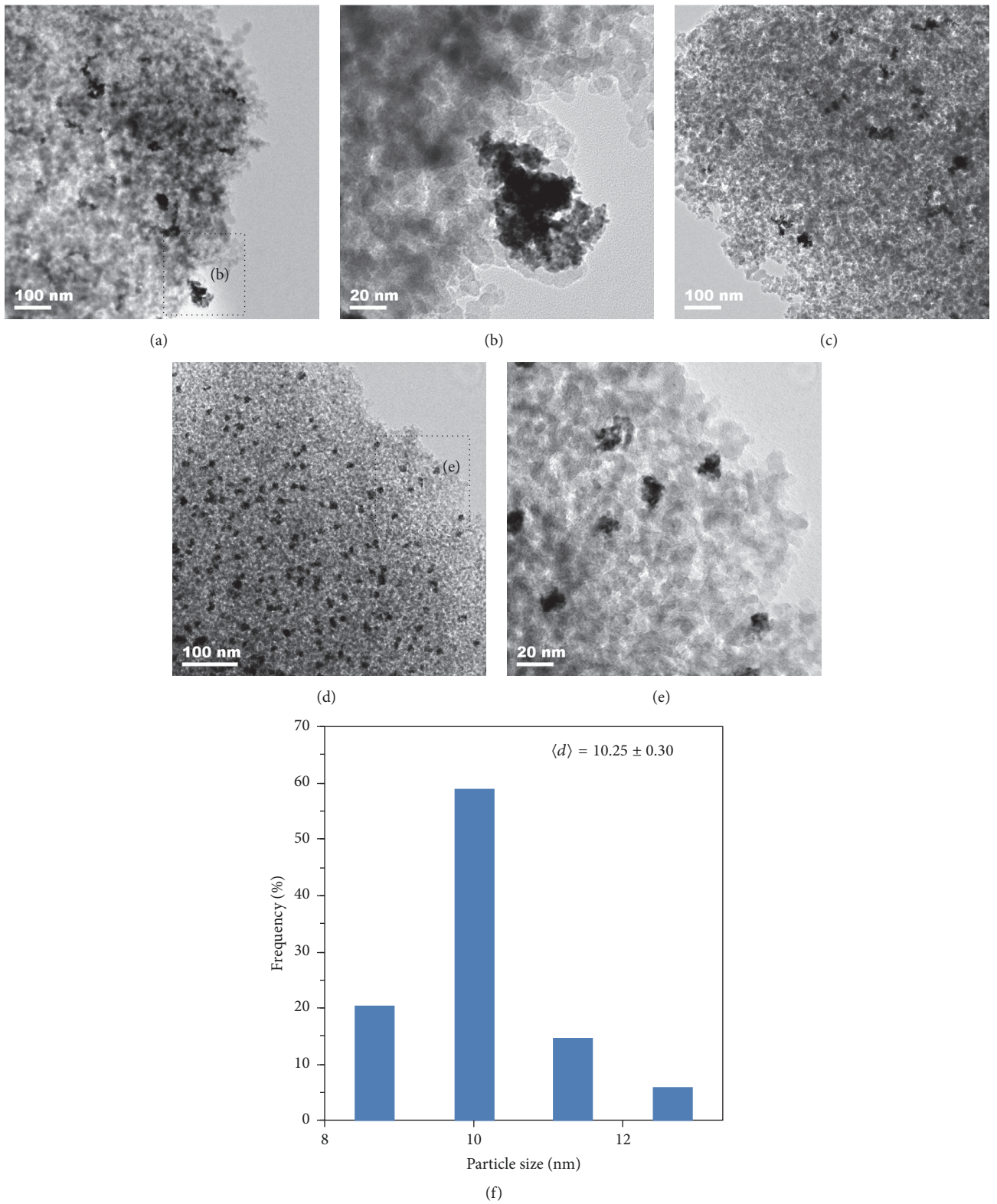

Figure 2: ((a), (b), and (c)) TEM images for the Pt/SiO_2 sample; ((d), (e)) TEM images and size distribution of particles for the $Pt\text{-}Cu/SiO_2$ sample. (f) is the size histogram of the particle distribution and the average size of the particles determined by statistical analysis of the TEM images; at least 50 individual crystallites were analyzed.

Table 2: Binding energies of the Pt 4f levels and the content of Pt species for the different catalysts.

Sample	Pt species	Pt species BE (eV)		Content of Pt species (%)
		$4f_{7/2}$	$4f_{5/2}$	
Pt/SiO_2	Pt^0	71.14	74.49	28
	Pt^{2+}	73.34	76.69	53
	Pt^{4+}	75.52	78.87	19
$Pt\text{-}Cu/SiO_2$	Pt^0	70.93	74.28	60
	Pt^{2+}	72.99	76.34	40

Table 3: Catalytic activities of Pt-Cu/SiO catalysts for the hydrogenation of CAL[a].

Sample	Con. (%)	TOF (h^{-1})[b]	Sel. (mol%)			
			COL	HALD	HALC	Others[c]
SiO_2	5.8	-	0	0.9	1.5	97.6
Cu/SiO_2	10.2	-	1.4	5.9	6.3	86.4
Pt/SiO_2	38.3	329	3.7	1.3	35.4	59.6
$Pt\text{-}Cu/SiO_2$	37.9	3076	64.1	5.4	11.3	19.2

[a]Reaction conditions: 50 mg catalyst, 1.00 g CAL, 30 mL isopropanol, 10 bar H_2, 80°C, 2 h. [b]Turnover frequency (TOF) = [moles of cinnamyl alcohol formed]/[(moles of Pt loading) × (reaction time) × D(Pt)] [27]. [c]Including possibly 1-(3-propoxyprop-1-enyl)benzene, cinnamyl formate, cinnamic acid, benzyl cinnamate, 4,4-diphenylcyclohexane-1,5-dienyl acetate, and other condensation products that could be identified by GC-MS because of their large molecular weights.

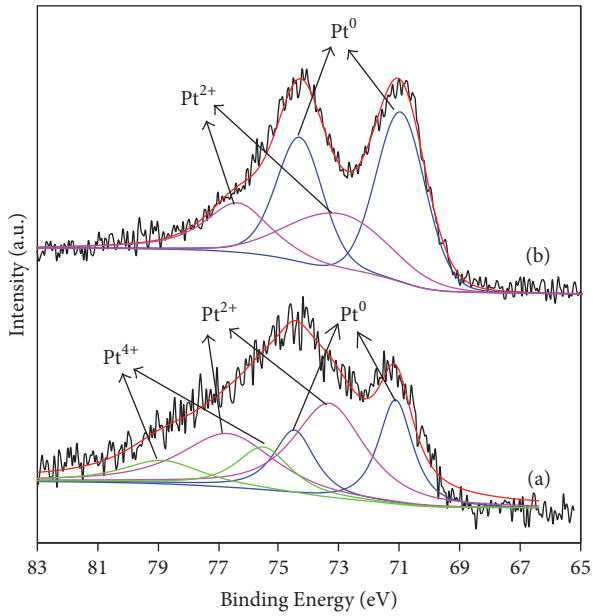

Figure 3: Pt 4f XPS spectra of (a) Pt/SiO_2 and (b) $Pt\text{-}Cu/SiO_2$.

3.2. Catalytic Performance. The selective hydrogenation of CAL was applied to evaluate the catalytic performance of the Pt/SiO_2 and $Pt\text{-}Cu/SiO_2$, and the results are shown in Table 3. It can be seen that SiO_2 and Cu/SiO_2 showed little activity to the selective hydrogenation of CAL. And Pt/SiO_2 showed 38.3% conversion of CAL, and the selectivity to COL, HALD, HALC, and other products was 3.7%, 1.3%, 35.4%, and 59.6%, respectively. 10.2% CAL could be converted over Cu/SiO_2, and the selectivity to COL, HALD, and HALC was 1.4%, 5.9%, and 9.3%, respectively. However, the $Pt\text{-}Cu/SiO_2$ catalyst performed 37.9% CAL conversion and 64.1% selectivity to COL, while the selectivity to HALC, HALD, and other side products was 5.4%, 11.3%, and 19.2%, respectively. And the TOF of Pt to form COL increased to 3076 h^{-1} from 329 h^{-1} for the Pt/SiO_2. Therefore, it is clear that the $Pt\text{-}Cu/SiO_2$ catalyst displays much higher selectivity to COL than Pt/SiO_2, while they showed similar conversion of CAL. This result is different from a past report supporting Pt and Cu on carbon nanotube by microwave-assisted polyol reduction [23]. The different results imply that the interaction between Pt and promoter may be different due to the distinctive preparation strategies. In this work, the enhanced selectivity to COL caused by promoter Cu could be attributed to the increased fraction of the metallic Pt^0 species on the surface of the $Pt\text{-}Cu/SiO_2$ catalyst. According to our previous studies, the amount of Pt^0 on the catalyst has a much larger influence on the selectivity of COL, while the Pt^{2+} and Pt^{4+} species are responsible for the high-molecular-weight secondary products [13, 20–22]. For Pt/SiO_2, there are more Pt^{2+} and Pt^{4+} species and less Pt^0 species, so it exhibits less selectivity to COL and higher selectivity to those condensation products. On the other hand, the $Pt\text{-}Cu/SiO_2$ catalyst possesses more Pt^0 species and less Pt^{2+} species on its surface; thus it displays much higher selectivity to COL than Pt/SiO_2.

4. Conclusions

The Pt-Cu bimetal catalyst was prepared on SiO_2 aerogel. The $Pt\text{-}Cu/SiO_2$ showed uniform Pt NPs benefitted from the introduction of Cu. The intensive interaction between Pt and Cu was observed in the $Pt\text{-}Cu/SiO_2$ catalyst, which results in the difference of Pt species on its surface and the electron transfer between Pt and Cu. The $Pt\text{-}Cu/SiO_2$ catalyst exhibited a remarkably enhanced selectivity to cinnamyl alcohol for the liquid-phase hydrogenation of cinnamaldehyde. This

promotion can be ascribed to the fact that Cu increases the amount of the Pt^0 species in the surface of the Pt-Cu/SiO_2 catalyst.

Conflicts of Interest

The authors declare no conflicts of interest.

Acknowledgments

This work was supported by Natural Sciences Fund of Heilongjiang Province (B2015009) and the Ph.D. Fund of Hanshan Normal University (no.QD20170503).

References

[1] P. Gallezot and D. Richard, "Selective hydrogenation of α,β-unsaturated aldehydes," *Catalysis Reviews*, vol. 40, no. 1-2, pp. 81–126, 1998.

[2] G. H. Wang, X. H. Deng, D. Gu et al., "Co_3O_4 nanoparticles supported on mesoporous carbon for selective transfer hydrogenation of α,β-unsaturated aldehydes," *Angewandte Chemie International Edition*, vol. 55, no. 37, pp. 11101–11105, 2016.

[3] D. Richard, P. Fouilloux, and P. Gallezot, "Characterization and metal catalysts," In Proceedings of the 9th International Congress on Catalysis, vol. 3, pp. 1074–1081, 1988.

[4] J. Liang, Z. B. Liang, R. Q. Zou, and Y. L. Zhao, "Heterogeneous catalysis in zeolites, mesoporous silica, and metal-organic frameworks," *Advanced Materials*, vol. 29, no. 30, 2017.

[5] T. Birchem, C. M. Pradier, Y. Berthier, and G. Cordier, "Reactivity of 3-methyl-crotonaldehyde on Pt(111)," *Journal of Catalysis*, vol. 146, no. 2, pp. 503–510, 1994.

[6] J. Teddy, A. Falqui, A. Corrias et al., "Influence of particles alloying on the performances of Pt-Ru/CNT catalysts for selective hydrogenation," *Journal of Catalysis*, vol. 278, no. 1, pp. 59–70, 2011.

[7] H. Vu, F. Gonçalves, R. Philippe et al., "Bimetallic catalysis on carbon nanotubes for the selective hydrogenation of cinnamaldehyde," *Journal of Catalysis*, vol. 240, no. 1, pp. 18–22, 2006.

[8] Y. S. Shi, Z. F. Yuan, Q. Wei, K. Q. Sun, and B. Q. Xu, "Pt-FeO_x/SiO_2 catalysts prepared by galvanic displacement show high selectivity for cinnamyl alcohol production in the chemoselective hydrogenation of cinnamaldehyde," *Catalysis Science and Technology*, vol. 6, no. 19, pp. 7033–7037, 2016.

[9] B. Wu, H. Huang, J. Yang, N. Zheng, and G. Fu, "Selective hydrogenation of α, β-unsaturated aldehydes catalyzed by amine-capped platinum-cobalt nanocrystals," *Angewandte Chemie*, vol. 124, no. 14, pp. 3496–3499, 2012.

[10] Q. Zheng, D. Wang, F. L. Yuan et al., "An effective Co-promoted platinum of Co–Pt/SBA-15 catalyst for selective hydrogenation of cinnamaldehyde to cinnamyl alcohol," *Catalysis Letters*, vol. 146, no. 8, pp. 1535–1543, 2016.

[11] Y. Gu, Y. H. Zhao, P. P. Wu, B. Yang, N. T. Yang, and Y. Zhu, "Bimetallic Pt_xCo_y nanoparticles with curved faces for highly efficient hydrogenation of cinnamaldehyde," *Nanoscale*, vol. 8, no. 21, pp. 10896–10901, 2016.

[12] S. Y. Song, X. C. Liu, J. Q. Li et al., "Confining the nucleation of Pt to in situ form (Pt-enriched cage)@CeO_2 Core@shell nanostructure as excellent catalysts for hydrogenation reactions," *Advanced Materials*, vol. 29, no. 28, 2017.

[13] X. W. Ji, X. Y. Niu, B. Li et al., "Selective hydrogenation of cinnamaldehyde to cinnamal alcohol over platinum/graphene catalysts," *ChemCatChem*, vol. 6, no. 11, pp. 3246–3253, 2014.

[14] K. R. Kahsar, D. K. Schwartz, and J. W. Medlin, "Control of metal catalyst selectivity through specific noncovalent molecular interactions," *Journal of the American Chemical Society*, vol. 136, no. 1, pp. 520–526, 2014.

[15] H. Rong, Z. Niu, Y. Zhao et al., "Structure Evolution and Associated Catalytic Properties of Pt- Sn Bimetallic Nanoparticles," *Chemistry - A European Journal*, vol. 21, no. 34, pp. 12034–12041, 2015.

[16] Z. Tian, X. Xiang, L. Xie, and F. Li, "Liquid-phase hydrogenation of cinnamaldehyde: Enhancing selectivity of supported gold catalysts by incorporation of cerium into the support," *Industrial & Engineering Chemistry Research*, vol. 52, no. 1, pp. 288–296, 2013.

[17] H. G. Manyar, B. Yang, H. Daly et al., "Selective hydrogenation of α,β-unsaturated aldehydes and ketones using novel manganese oxide and platinum supported on manganese oxide octahedral molecular sieves as catalysts," *ChemCatChem*, vol. 5, no. 2, pp. 506–512, 2013.

[18] J. P. Lai, R. Luque, and G. B. Xu, "Recent advances in the synthesis and electrocatalytic applications of Platinum-based bimetallic alloy nanostructures," *ChemCatChem*, vol. 7, no. 20, pp. 3206–3228, 2015.

[19] H. L. Liu, F. Nosheen, and X. Wang, "Noble metal alloy complex nanostructures: controllable synthesis and their electrochemical property," *Chemical Society Review*, vol. 44, no. 10, pp. 3056–3078, 2015.

[20] Q. Han, Y. Liu, D. Wang, F. Yuan, X. Niu, and Y. Zhu, "Effect of carbon nanosheets with different graphitization degrees as a support of noble metals on selective hydrogenation of cinnamaldehyde," *RSC Advances*, vol. 6, no. 100, pp. 98356–98364, 2016.

[21] Y. J. Zhu and F. Zaera, "Selectivity in the catalytic hydrogenation of cinnamaldehyde promoted by Pt/SiO_2 as a function of metal nanoparticle size," *Catalysis Science and Technology*, vol. 4, no. 4, pp. 955–962, 2014.

[22] D. Wang, Y. Zhu, C. Tian et al., "Synergistic effect of Mo_2N and Pt for promoted selective hydrogenation of cinnamaldehyde over Pt-Mo_2N/SBA-15," *Catalysis Science and Technology*, vol. 6, no. 7, pp. 2403–2412, 2016.

[23] Z. Guo, Y. Chen, L. Li, X. Wang, G. L. Haller, and Y. Yang, "Carbon nanotube-supported Pt-based bimetallic catalysts prepared by a microwave-assisted polyol reduction method and their catalytic applications in the selective hydrogenation," *Journal of Catalysis*, vol. 276, no. 2, pp. 314–326, 2010.

[24] K. Joseph Antony Raj, M. G. Prakash, T. Elangovan, and B. Viswanathan, "Selective hydrogenation of cinnamaldehyde over cobalt supported on alumina, silica and titania," *Catalysis Letters*, vol. 142, no. 1, pp. 87–94, 2012.

[25] J. J. F. Scholten, A. P. Pijpers, and M. L. Hustings, "Surface characterization of supported and nonsupported hydrogenation catalysts," *Catalysis Reviews: Science and Engineering*, vol. 27, no. 1, pp. 151–206, 1985.

[26] A. J. Plomp, H. L. Vuori, A. O. I. Krause, K. P. de Jong, and J. H. Bitter, "Particle size effects for carbon nanofiber supported platinum and ruthenium catalysts for the selective hydrogenation of cinnamaldehyde," *Applied Catalysis A: General*, vol. 351, no. 1, pp. 9–15, 2008.

[27] B. F. MacHado, S. Morales-Torres, A. F. Pérez-Cadenas et al., "Preparation of carbon aerogel supported platinum catalysts

for the selective hydrogenation of cinnamaldehyde," *Applied Catalysis A: General*, vol. 425-426, pp. 161–169, 2012.

[28] J. Yang, Y. Xie, R. Wang et al., "Synergistic effect of tungsten carbide and palladium on graphene for promoted ethanol electrooxidation," *ACS Applied Materials & Interfaces*, vol. 5, no. 14, pp. 6571–6579, 2013.